THE JOURNAL OF BIOLOGICAL CHEMISTRY VOL. 286, NO. 39, pp. 33747–33758, September 30, 2011

β-Amyloid Peptide Variants in Brains and Cerebrospinal Fluid from Amyloid Precursor Protein (APP) Transgenic Mice

COMPARISON WITH HUMAN ALZHEIMER AMYLOID[*] [S]

Received for publication, April 1, 2011, and in revised form, July 13, 2011 Published, JBC Papers in Press, July 27, 2011, DOI 10.1074/jbc.M111.246561

Heinke Schieb[‡], Hartmut Kratzin[§], Olaf Jahn[§], Wiebke Möbius[¶], Sabine Rabe[‖], Matthias Staufenbiel[‖], Jens Wiltfang[‡], and Hans W. Klafki[‡1]

From the [‡]Department of Psychiatry and Psychotherapy, LVR-Klinikum, Essen, University of Duisburg-Essen, D-45147 Essen, Germany, the [§]Proteomics Group, Max-Planck-Institute of Experimental Medicine, D-37075 Göttingen, Germany, the [¶]Department of Neurogenetics, Max-Planck-Institute of Experimental Medicine, D-37075 Göttingen, Germany, and the [‖]Novartis Institutes for BioMedical Research, CH-4002 Basel, Switzerland

In this study, we report a detailed analysis of the different variants of amyloid-β (Aβ) peptides in the brains and the cerebrospinal fluid from APP23 transgenic mice, expressing amyloid precursor protein with the Swedish familial Alzheimer disease mutation, at different ages. Using one- and two-dimensional gel electrophoresis, immunoblotting, and mass spectrometry, we identified the Aβ peptides Aβ(1–40), -(1–42), -(1–39), -(1–38), -(1–37), -(2–40), and -(3–40) as well as minor amounts of pyroglutamate-modified Aβ (Aβ(N3pE)) and endogenous murine Aβ in brains from 24-month-old mice. Chemical modifications of the N-terminal amino group of Aβ were identified that had clearly been introduced during standard experimental procedures. To address this issue, we additionally applied amyloid extraction in ultrapure water. Clear differences between APP23 mice and Alzheimer disease (AD) brain samples were observed in terms of the relative abundance of specific variants of Aβ peptides, such as Aβ(N3pE), Aβ(1–42), and N-terminally truncated Aβ(2/3–42). These differences to human AD amyloid were also noticed in a related mouse line transgenic for human wild type amyloid precursor protein. Taken together, our findings suggest different underlying molecular mechanisms driving the amyloid deposition in transgenic mice and AD patients.

The major histopathological hallmarks of Alzheimer disease (AD)[2] are neuritic plaques and neurofibrillary tangles that are composed of aggregates of the amyloid-β (Aβ) peptide and hyperphosphorylated Tau protein, respectively (1–5). Aβ peptides are generated from the amyloid precursor protein (APP) by two proteolytic enzymes called β- and γ-secretases (for reviews see Refs. 6–8). The resulting Aβ peptides represent a heterogeneous group of peptides with different lengths. Aβ(1–40) is the predominant form released from cultured cells (9) and in biological fluids, such as blood (10) and cerebrospinal fluid (CSF) (11). Longer forms ending at amino acid 42 are believed to be particularly important in the pathogenesis of AD due to a higher propensity to aggregate (12). Aβ accumulation in the AD brain likely starts many years before cognitive deficits become evident (13, 14). The reported inverse association of *in vivo* cortical binding of Pittsburgh Compound-B and CSF Aβ42 suggests that brain amyloid deposition and low CSF Aβ42 are mechanistically related (13, 15). Based on the amyloid cascade hypothesis stating a central role of Aβ in AD, several therapeutic strategies targeting Aβ and aiming for inhibition of disease progression are pursued. The more advanced of these potential therapeutic approaches include inhibition or modulation of cellular Aβ production and Aβ-targeted immunotherapy (16, 17).

Animal models of the human disease are important research tools to facilitate the study of the pathophysiology, and they have been widely used for testing potential therapeutic approaches. The APP23 mouse line (18) represents one out of several well established transgenic mouse models that display key features of the amyloid pathology observed in patients with Alzheimer disease (for review, see Ref. 19). Human APP751 carrying the Swedish double mutation (K670N/M671L) is overexpressed in APP23 mice under control of the murine *Thy-1* promoter, which drives neuron-specific expression (20). At ~6 months of age, the first amyloid deposits are observed in heterozygous animals (18).

We present here a detailed immunoblot and mass spectrometry analysis of the different variants of Aβ peptides that can be detected after one- and two-dimensional electrophoretic separation in brain extracts and CSF from heterozygous APP23 mice at different ages. In addition to standard amyloid preparation with formic acid, extraction in pure water was applied for preparing amyloid fibrils in the absence of potentially modifying agents (21). Our study reveals clear differences between APP23 mice and human AD brain samples in terms of the relative abundance of specific variants of Aβ peptides. To explore whether the observed differences might be attributed to the

* This work was supported by European Union cNEUPRO Contract LSHM-CT-2007-037950, NeuroTAS Contract LSHB-CT-2006-037953, and by Grant PURE (Protein Research Unit Ruhr within Europe) from the State Government of North Rhine-Westphalia.

[S] The on-line version of this article (available at http://www.jbc.org) contains supplemental Figs. S1 and S2, "Experimental Procedures," and additional references.

[1] To whom correspondence should be addressed: Laboratory of Molecular Neurobiology, Dept. of Psychiatry and Psychotherapy, LVR-Klinikum Essen, University of Duisburg-Essen, Virchowstr. 171, 45147 Essen, Germany. Tel.: 49-201-723-4225; Fax: 49-201-723-5543; E-mail: hans.klafki@uni-due.de.

[2] The abbreviations used are: AD, Alzheimer disease; Aβ, β-amyloid; APP, amyloid precursor protein; CSF, cerebrospinal fluid; IEF, isoelectric focusing; IPG, immobilized pH gradient; bis-Tris, 2-[bis(2-hydroxyethyl)amino]-2-(hydroxymethyl)propane-1,3-diol; Bicine, *N,N*-bis(2-hydroxyethyl)glycine.

TABLE 1

Demographic and neuropathological data for the human donors

The demographic data, apoE status, and neuropathological diagnosis according to Braak and Braak (37, 55) were provided by the Netherlands Brain Bank, Netherlands Institute for Neuroscience, Amsterdam.

	Neuropathological diagnosis	Braak stage	Braak stage for amyloid	Age	Sex	ApoE status
AD1	Alzheimer disease	6	C	76	Female	ε4/ε2
AD2	Alzheimer disease	6	[a]	88	Female	ε4/ε3
AD3	Alzheimer disease	5	C	79	Male	ε3/ε3
NDC1	Nondemented control	1	B	77	Female	ε4/ε3
NDC2	Nondemented control	1	0	78	Male	ε4/ε3

[a] For this individual, a Braak stage for amyloid was not explicitly indicated. However, according to the information provided, "classical senile plaques were rather frequent."

expression and processing of a familial Alzheimer disease mutant APP form, we furthermore investigated brain extracts and CSF from APP51 mice that are transgenic for human wild type APP751 (22).

EXPERIMENTAL PROCEDURES

Transgenic Mice—The transgenic mice investigated express the human APP751 isoform under the control of the murine *Thy-1* promoter. The mice were on a C57BL/6 background and were hemizygous for the transgene. Only male mice were included in this study. APP23 mice express APP with the KM670/671NL "Swedish" mutation (18), whereas APP51 mice express APP wild type (22). All animal experiments were in compliance with protocols approved by the Swiss Animal Care and Use Committees. CSF was collected from the cisterna magna under anesthesia with 3% isoflurane. Thereafter, the mice were decapitated, and the brains were removed, frozen on dry ice, and stored at −80 °C until used.

Human Samples—The human brain tissue was obtained from The Netherlands Brain Bank, Netherlands Institute for Neuroscience, Amsterdam. All material was collected from donors for or from whom a written informed consent for a brain autopsy and the use of the material and clinical information for research purposes had been obtained by the Netherlands Brain Bank. Three of the five donors used for the study were neuropathologically diagnosed with Alzheimer disease and the other two were diagnosed as nondemented controls. The post-mortem delay ranged between 3 h, 40 min and 5 h, 30 min. Demographic data and neuropathological findings provided by the Netherlands Brain Bank are summarized in Table 1.

Amyloid Extraction from Brain Tissue—Brain samples were weighed and homogenized by sonication in 1 ml per 100 mg wet tissue of a triple detergent buffer (50 mM HEPES, pH 7.4, 150 mM NaCl, 1.0% Nonidet P-40 ("Igepal CA 630") (v/v), 0.5% sodium deoxycholate (w/v), 0.1% SDS (w/v), and "Complete" protease inhibitor mixture (Roche Applied Science), 1 tablet per 10 ml). After centrifugation (16,000 × *g*, 15 min, 4 °C), the supernatant was collected, and the protein concentration was determined by the BCA assay. The pellet was washed twice with PBS and resolubilized under shaking for 20 min at room temperature with 70% formic acid (150 μl per 100 mg of wet brain tissue). After centrifugation (16,000 × *g*, 10 min, 4 °C), the supernatant was collected, and the formic acid was evaporated in a vacuum concentrator. The formic acid-soluble material was then resolved under shaking for 10 min at 95 °C in 50 μl of SDS sample buffer (0.36 M bis-Tris, 0.16 M Bicine, 1% SDS (w/v), 15% sucrose (w/v), and 0.0075% bromphenol blue (w/v); 50 μl per 100 mg wet brain tissue). Insoluble material was removed by centrifugation, and the supernatant was collected as the formic acid fraction. In an additional control experiment, stable isotope-labeled synthetic Aβ(1–40) containing Arg($^{13}C_6/^{15}N_4$) and Lys($^{13}C_6/^{15}N_2$) (ClearPoint, Anaspec, Fremont, CA) was added to the detergent-insoluble pellet before extraction with 70% formic acid. Alternatively, amyloid fibrils from brain samples were extracted essentially according to Pras *et al.* (21). Briefly, the brain tissue samples were first homogenized by sonication in 1 ml per 100 mg wet tissue of saline (150 mM NaCl, 2 mM Tris-HCl, pH 7.4, protease inhibitor mixture) to extract soluble proteins. The insoluble material was pelleted by centrifugation at 4 °C and 16,000 × *g* for 30 min, and the procedure was repeated until no further changes in the UV absorption at 280 nm of the supernatants were observed. The insoluble material was then homogenized in ultrapure water (1 ml per 100 mg wet tissue) and centrifuged as described above. Again, this step was repeated until no further amyloid material could be extracted as indicated by a stable UV absorption at 280 nm.

Negative Staining of Amyloid Fibrils—Two different protocols were used for negative staining of β-amyloid water extracts from an APP23 mouse brain sample. First, a drop of protein solution was diluted 1:1 with 0.2% glutaraldehyde in water and immediately incubated with a Formvar-coated 100 hexagonal mesh copper EM grid (Plano, Germany) for 15 s. After removing the fluid from the grid with a pointed piece of filter paper, the grid was rinsed shortly on three droplets of water and incubated 15 s with 2% (w/v) uranyl acetate (SPI Supplies). Subsequently, the fluid was again removed with pointed filter paper, and the grid was dried. In the second approach, 9 μl of water extract were placed on an EM grid and incubated 5 min after adding 1 μl of 100 mM $CaCl_2$ in water. After removing excess fluid with filter paper, the grid was stained for 5 min with 1% (w/v) phosphotungstic acid (Merck) and adjusted to pH 5.7 with 1 M NaOH according to Ref. 23. Grids were analyzed with a LEO EM912 Omega (Zeiss, Oberkochen), and digital micrographs were obtained with an on-axis 2048 × 2048-CCD camera (Proscan, Scheuring).

Immunoprecipitation of Aβ Peptides—Magnetic sheep anti-mouse-IgG Dynabeads M-280 were precoated with the monoclonal antibody 1E8 (Bayer Schering Pharma AG, Berlin, Germany) (40 μg/ml) according to the manufacturer's protocol (Dynal, Hamburg, Germany). Equal protein amounts in a 1-ml volume were mixed with 250 μl of a 5-fold concentrated detergent buffer yielding final concentrations of 50 mM HEPES, 150 mM NaCl, 0.5% Nonidet P-40 (v/v), 0.25% sodium deoxycholate (w/v), 0.05% SDS (w/v). 30 μl of 1E8-coated magnetic beads were added, and immunoprecipitation was performed under rotation for 15 h at 4 °C. Subsequently, the beads were washed three times for 5 min with PBS, 0.1% bovine serum albumin (w/v) and once for 3 min with 10 mM Tris-HCl, pH 7.5. To elute bound Aβ peptides, the sample was heated to 95 °C for 5 min in 25 μl of sample buffer (0.36 M bis-Tris, 0.16 M Bicine, 1% SDS (w/v), 15% sucrose (w/v) and 0.0075% bromphenol blue (w/v)).

Bicine/bis-Tris/Tris/Sulfate SDS-PAGE—For the analysis of Aβ peptides the Bicine/bis-Tris/Tris/sulfate SDS-PAGE was used (24). To separate the different C-terminal Aβ peptide variants, the urea version of the gel system was applied (25, 26). The percentage of total acrylamide plus bisacrylamide (w/v) in the separation gel was 10%, and gel thickness was 0.5 mm. The gels were run at room temperature for 50 min at a constant current of 25 mA/gel. Each gel carried a dilution series of a synthetic standard Aβ peptide mix.

Two-dimensional Aβ-immobilized pH Gradient (IPG)-PAGE—IPG electrofocusing was performed with dry IPG strips (GE Healthcare) on an Ettan™ IPGphor™ II isoelectric focusing (IEF) system (GE Healthcare). IPG strips were rehydrated in rehydration solution (8.3 M urea, 2% CHAPS (w/v), 0.5% (v/v) Pharmalyte pH 3–10, 20 mM DTT) containing the sample for 10 h at 20 °C. IEF was performed as described elsewhere (27). For the urea-free IEF version, the rehydration solution was modified to 4% CHAPS (w/v), 0.5% Pharmalyte (v/v) pH 3–10, 20 mM DTT. After focusing, IPG strips were placed on a 1-mm thick Aβ-SDS-polyacrylamide gel and embedded by a low melting agarose solution (1% low-melt agarose (w/v), 0.36 M bis-Tris, 0.16 M Bicine, 0.25% SDS, 0.002% bromphenol blue (w/v)). A Teflon spacer was inserted next to the IPG strip to form a one-dimensional slot for synthetic Aβ standards. Gels were run at a constant current of 15 mA per gel for 10 min, followed by 25 mA per gel for 10 min and continued with 35 mA per gel until the running front reached the bottom of the gel. Strip holders that had been used for IEF of large amounts of Aβ peptides were subjected to a harsh cleaning procedure, including prolonged treatment with proteinase K to avoid cross-contaminations in subsequent experiments (28).

Immunoblot Analysis and Quantification—The separated Aβ peptides were transferred onto Immobilon-P PVDF membranes at 1 mA/cm^2 under semidry conditions (Hoefer Semi-Phor) for 30 min (0.5-mm thick gels) or 45 min (1.0-mm thick gels) (26). The PVDF membranes were then boiled for 3 min in PBS in a microwave oven to improve antibody binding (29). Immunostaining with the monoclonal Aβ-antibodies 1E8 (Bayer Schering Pharma AG, Berlin, Germany) and 6E10 (Covance, Emeryville, CA) was performed as described before (30). For the detection of Aβ(N3pE) peptides, the blots were blocked in RotiBlock (Carl Roth GmbH, Karlsruhe, Germany) and incubated overnight at 4 °C with the polyclonal antibody amyloid β (N3pE) (IBL, Hamburg, Germany) at a concentration of 0.5 μg/ml. The next day, the blots were washed three times in 0.075% Tween in PBS and were probed with peroxidase-coupled goat anti-rabbit IgG (1:50,000 in PBS-T). All blots were developed with ECL-Plus™ chemiluminescent substrate according to the manufacturer's instructions (GE Healthcare) and detected with an Intas Imager (Intas, Göttingen, Germany). Band intensities were quantified with the Quantity One Software 4.1 (Bio-Rad) relative to a dilution series of Aβ(1–40) present in a mixture of Aβ standard peptides. The mouse brain extracts were prediluted to reach final Aβ concentrations that were in the range of the Aβ(1–40) calibration curve. Each mouse brain extract was analyzed on two separate blots, and the mean values were calculated from the duplicates.

Gel Staining—For Coomassie staining of two-dimensional gels, a modified version of the "Blue Silver" method (31) was used. Gels were first fixed for 1 h at room temperature in fixation solution (30% ethanol, 2% phosphoric acid) and then stained for 16 h at room temperature in Coomassie staining solution (0.12% Coomassie Brilliant Blue G-250 (w/v), 20% ethanol (v/v), 10% ammonium sulfate (w/v), 10% phosphoric acid (v/v)). The next day the gel was washed several times in 20% ethanol.

Mass Spectrometry of Intact Aβ—For mass spectrometric analyses, the spots of interest were excised from Coomassie-stained two-dimensional gels and extracted with a mixture of ammonia (25%)/water/isopropyl alcohol, 1:3:2 (v/v/v). For extraction, the thoroughly minced gel pieces suspended in 50 μl of solvent were vortexed at 37 °C for 1 h, ultrasonicated in an ultrasonication bath for 10 min, and finally centrifuged. After removal of the supernatant, the procedure was repeated with another 50 μl of solvent, and the remainder was extracted with 50 μl of ethanol. The combined extracts were concentrated and used for MALDI mass spectrometry in the linear mode on a Bruker Ultraflex TOF/TOF mass spectrometer. Therefore, the samples were applied to AnchorChip targets (Bruker, Germany) using the dried droplet method with 2,5-dihydroxybenzoic acid as the matrix.

Statistical Analysis—Statistical tests were performed with GraphPad Prism 5.01 software (GraphPad Software Inc. La Jolla, CA). A level of $p < 0.05$ was regarded as statistically significant; the actual p levels are given for descriptive purposes.

RESULTS

Age-dependent Aβ Accumulation in the Brains of APP23 Mice—Hemibrains from 3-, 7-, 15-, and 24- month-old APP23 transgenic mice were extracted first with an extraction buffer containing 0.1% SDS, 1.0% Nonidet P-40, and 0.5% sodium deoxycholate to prepare the detergent-soluble fraction. In a second step, the remaining insoluble material was extracted with 70% formic acid to obtain the formic acid fraction. The samples were separated by SDS-PAGE in the presence of urea and analyzed by immunoblot with the monoclonal antibody 1E8. On immunoblots, this antibody recognizes Aβ peptides starting with Asp-1 or Ala-2 (30). One-dimensional separation revealed five different forms of Aβ that were tentatively identified as Aβ(1–37), -(1–38), -(1–39), -(1–40), and -(1–42) according to their electrophoretic mobilities (Fig. 1*A*). The amount of the Aβ peptides in the different fractions was estimated from the blots by semi-quantitative image analysis and in comparison with a standard curve obtained with synthetic Aβ(1–40). Detergent-soluble Aβ was found in all tested brain samples, and its total amount increased substantially between 7 and 24 months of age. Detergent-insoluble Aβ was not detected in mice younger than 7 months. The total amount of Aβ in the formic acid fraction augmented dramatically between 7 and 24 months of age (Table 2).

In all Aβ-positive detergent and formic acid fractions and independent of age, the most prominent of the different Aβ variants was Aβ(1–40) (Fig. 1*A*). To evaluate the relative contribution of Aβ(1–42), which is known to be particularly prone to aggregation (32), the Aβ(1–42)/(1–40) ratio was calculated.

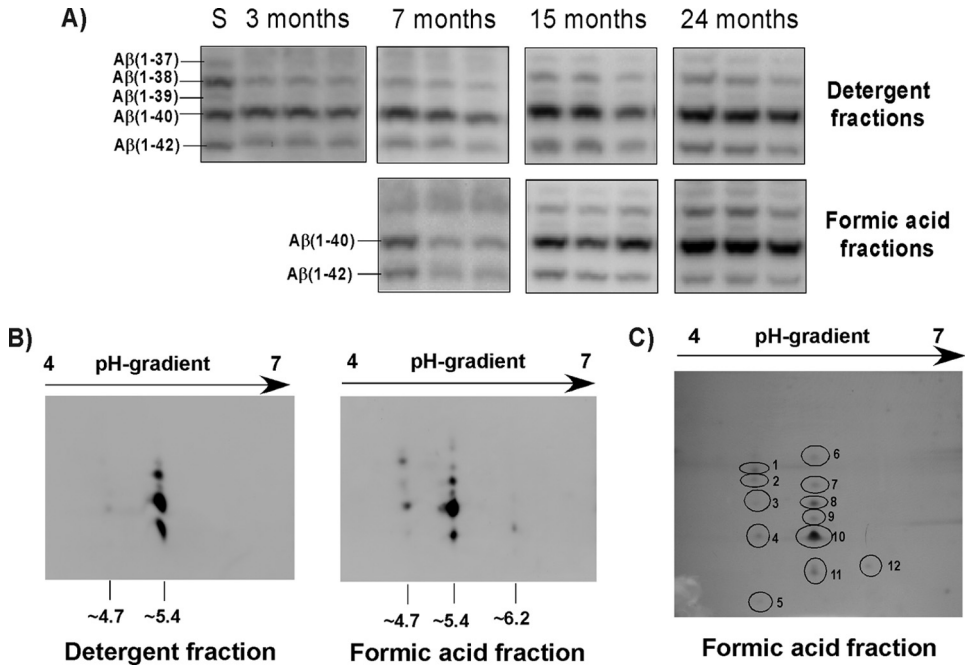

FIGURE 1. **Aβ peptide variants in APP23 mice.** *A,* representative Aβ peptide blots are shown. Samples are derived from detergent and formic acid fractions of APP23 mouse brains at different ages. Aβ peptides were separated by urea-SDS-PAGE followed by immunoblot with mAb 1E8. The total protein amount loaded for the different age groups was adjusted to obtain comparable signals on the blots (detergent fractions: 10 μg for 3 months and 7 months, 500 ng for 15 months, and 100 ng for 24 months; formic acid fractions: 5 μl of a 1:10, a 1:2000, or a 1:10,000 dilution for 7-, 15-, and 24-month-old mice, respectively). *S,* mixture of synthetic Aβ peptides. *B,* representative two-dimensional Western blots of detergent and formic acid fractions from the brain of a 24-month-old APP23 mouse. IPG strips with a linear pH gradient from 4 to 7 were used. The estimated pI values of the observed Aβ peptides are indicated. The figure shows those sections of the two-dimensional separations in which the Aβ peptides were resolved. *C,* Coomassie-stained two-dimensional gel of formic acid-extracted Aβ peptides from the brain of a 24-month-old APP23 mouse. The spots that were excised for mass spectrometric analysis are *encircled*. The *numbers* correspond to those in Table 3.

TABLE 2
Total Aβ and Aβ(1–42)/(1–40) ratios in the detergent- and formic acid brain extracts from APP23 mice at different ages

	Total Aβ (ng/mg wet tissues)[a]				Aβ(1–42)/(1–40) ratio			
	Detergent fraction		Formic acid fraction		Detergent fraction		Formic acid fraction	
Age	Median	25–75% percentile	Median	25–75% percentile	Median	25–75% percentile	Median	25–75% percentile
months								
3 (n = 4)	0.42	0.39–0.45			0.26	0.22–0.28		
7 (n = 5)	0.63	0.56–0.68	0.06	0.04–0.12	0.30	0. 27–0.32	0.67	0.61–0.82
15 (n = 5)	42.50	32–54	56.42	39–75	0.28	0.25–0.32	0.20	0.14–0.26
24 (n = 8)	458.90	369–552	338.20	267–352	0.17	0.14–0.19	0.06	0.06–0.07

[a] Brain tissue samples were subjected to Aβ urea-SDS-PAGE followed by immunoblot with the mAb 1E8. The blots were run in duplicate, and the Aβ peptides were quantified by comparison with a dilution series of synthetic Aβ(1–40) standards. The values for the distinct Aβ variants were added to obtain total Aβ. For each group, medians and 25–75% percentiles are shown. The statistical significance between age groups (rank sums) was analyzed with the nonparametric Kruskal-Wallis test and Dunn's multiple comparison post-test. The Aβ(1–42)/(1–40) ratio in the detergent fractions from 24-month-old mice was statistically significantly lower than in 7- and 15-month-old mice ($p < 0.01$ for 24 months *versus* 7 months, and $p < 0.05$ for 24 months *versus* 15 months, respectively). In the formic acid fractions, the Aβ(1–42)/(1–40) ratio was statistically significantly lower in 24-month-old animals than in 7-month-old mice ($p < 0.001$).

In the detergent fractions, the median Aβ(1–42)/(1–40) ratio remained stable at ~0.3 between 3 and 15 months of age and decreased to ~0.17 in 24-month-old mice. In the formic acid fractions, the median Aβ(1–42)/(1–40) ratio was ~0.7 in 7-month-old mice, representing an early plaque amyloid stage, and decreased with age to ~0.06 in 24-month-old mice ($p <$ 0.001, Kruskal-Wallis Test followed by Dunn's multiple comparison post-test) (Table 2).

Additional Aβ peptide variants displaying shifts in their pI values were revealed by two-dimensional urea-SDS-PAGE followed by immunoblot analysis. Fig. 1*B* shows examples of two-dimensional immunoblots of detergent and formic acid extracts from a 24-month-old APP23 mouse. Major Aβ variants detected by mAb 1E8 displayed a pI of ~5.4. In addition, Aβ peptides with estimated pI values of ~6.2 or ~4.7 were regularly observed in the formic acid fractions and, to a smaller extent, also in the detergent extracts from 24-month-old APP23 mice.

Mass Spectrometric Characterization of Aβ Variants in Formic Acid Fractions—To provide unequivocal identification of the Aβ peptides isolated from the brains of 24-month-old APP23 mice and to search for possible chemical peptide modifications, we applied different mass spectrometric methods. To this end, intact Aβ peptides were extracted from spots that were excised from Coomassie-stained two-dimensional gels (Fig. 1*C*). Compared with immunoblots, the general Coomassie staining revealed only one additional peptide spot (*spot 5* in Fig. 1*C*) in the region of the two-dimensional gel where Aβ peptides were expected. The gel extracts were subjected to MALDI-TOF MS, which allowed the assignments shown in Table 3. Most of

TABLE 3
Molecular masses of the Aβ peptides extracted with 70% formic acid from brains of 24-month-old APP23 mice

Estimated pI	Spot[a]	Proposed Aβ peptide	M_r calculated	M_r observed
4.7	1	Aβ(1–40) + 28	4357.9	4357.9
		Aβ(1–40) + 43	4372.9	4373.6
	2	Aβ(1–40) + 28	4357.9	4356.7
		Aβ(1–40) + 43	4372.9	4372.9
	3	Aβ(1–38) + 28	4159.6	4160.2
		Aβ(1–38) + 43	4174.6	4175.9
	4	Aβ(1–40) + 28	4357.9	4356.5
		Aβ(1–40) + 43	4372.9	4372.0
	5	Mouse Aβ(1–40)	4233.8	4235.8
5.4	6	Aβ(1–40)ox*	4345.8	4346.8
	7	Aβ(1–37)	4074.5	4075.2
	8	Aβ(1–38)	4131.6	4131.5
	9	Aβ(1–39)	4230.7	4230.2
	10	Aβ(1–40)	4329.9	4329.4
	11	Aβ(1–42)	4514.1	4515.9
6.2	12	Aβ(2–40)	4214.8	4216.8
		Aβ(3–40)	4143.7	4145.6

[a] The spots were numbered according to Fig. 1*C*. Several Aβ peptides were found with and without oxidation at methionine as indicated by a mass difference of 16. For the sake of clarity, however, only the observed masses of nonoxidized peptides are listed except for Aβ(1–40)ox*, which was most likely oxidized prior to separation (see text).

the peptides were found with and without oxidation at methionine in position 35 as indicated by a mass difference of 16. The most prominent spot in the formic acid extracts from the brains of APP23 mice was the Aβ(1–40) peptide with a pI of ~5.4 and a measured mass of 4329.4 (calculated mass 4329.9). Other spots displaying a pI of ~5.4 were identified as Aβ(1–42), -(1–39), -(1–38), and -(1–37). *Spot 6* from Fig. 1*C* contained an oxidized form of the Aβ(1–40) peptide and was designated Aβ(1–40)ox*. This peptide migrated above all other Aβ spots, which is consistent with the finding that oxidized Aβ peptides have a retarded electrophoretic mobility under these conditions (33, 34). Accordingly, Aβ(1–40)ox* was most probably oxidized before the electrophoretic separation. Other Aβ peptides were presumably partially oxidized during experimental procedures, *e.g.* electrophoresis, fixation, staining, spot extraction, or MS analysis. The N-terminally truncated peptides Aβ(2–40) and -(3–40) migrated as a single spot at an estimated pI of ~6.2 (*spot 12* in Fig. 1*C* and Table 3). The shifted pI value can be easily explained by the absence of the aspartic acid residue Asp-1. Several additional peptide spots displayed a more acidic pI of ~4.7. Spot 5 migrated faster than all other peptides. It was detected by Coomassie staining but not on immunoblots probed with the mAb 1E8, which is directed against human Aβ. For this peptide, we obtained a measured mass of 4235.8, which is in reasonable agreement with the theoretical mass of 4233.8 for endogenous mouse Aβ(1–40). The masses we observed for the remaining peptides displaying an acidic pI shift indicated the presence of modified forms of human Aβ(1–40) and Aβ(1–38), with mass differences of +28 or +43 (Table 3).

By mass spectrometric sequencing, the underlying chemical modifications could be unequivocally assigned to the N terminus of Asp-1 and were identified as formylation (+28) and carbamoylation (+43), respectively (supplemental Fig. S1). To further explore whether *N*-formylation and *N*-carbamoylation of Aβ had occurred artificially during the experimental procedures, we repeated the sequential amyloid extraction from the brain of a 24-month-old APP23 mouse and added stable isotope-labeled Aβ as an internal standard prior to the addition of formic acid. Formylation (+28) and carbamoylation (+43) of the N-terminal Lys-C fragment were found in both the human Aβ from the APP23 mouse and in the stable isotope-labeled internal standard (supplemental Fig. S2). Thus, the observed modifications had occurred at the stages of extraction (formylation by formic acid) and separation (carbamoylation by urea) and therefore have to be considered experimental artifacts. A fraction of the N-terminal Lys-C fragments from the pI ~4.7 Aβ was apparently unmodified.

Characterization of Amyloid Prepared in Water—As a more gentle approach to the preparation of amyloid, we additionally employed a method that was first described by Pras *et al.* (21) for the isolation of amyloid fibrils from the spleen of a patient with primary amyloidosis. In brief, following the removal of proteins soluble in saline, the amyloid fibrils were extracted from APP23 mouse brain by repeated homogenization in deionized ultrapure water. Fig. 2*A* shows the UV absorptions of the saline and the water fractions and Fig. 2*B* the corresponding immunoblot analysis. As expected, Aβ peptides were found in the initial saline extracts, representing a highly soluble fraction. Only trace amounts of Aβ peptides were detected in the first extract prepared in ultrapure water, which presumably still contained substantial amounts of ions. Appreciable amounts of deposited Aβ peptides were finally extracted in the water fractions 2–5. This elution pattern for amyloid is in agreement with the original report by Pras *et al.* (21). One defining general feature of amyloid, irrespective of the specific amyloid protein under investigation, is the fibrillar ultrastructure revealed by electron microscopy (35, 36). In the water extract from an APP23 mouse brain, we could observe negatively stained coiled fibrils by electron microscopy, confirming that the Aβ peptides in the water extract most probably represented fibrillar amyloid (Fig. 2*C*). Two-dimensional immunoblot analysis of the second water fraction revealed a pattern of Aβ variants that was similar to the formic acid fraction and contained N-terminally truncated (pI ~6.2) Aβ forms as well as variants displaying an acidic pI shift (pI ~4.7) (Fig. 2*D*). To further exclude the possibility of artificial carbamoylation, we subjected an aliquot of water extracted amyloid to isoelectric focusing in the absence of urea followed by SDS-PAGE (without urea) and immunoblot analysis. In the absence of urea, the C-terminal Aβ variants are not resolved in the second dimension (25, 26). Again, a major fraction of Aβ with a pI of ~5.4 and minor amounts of additional Aβ peptides displaying either more alkaline or more acidic pI values were detected (Fig. 2*E*). Our attempts to determine the masses of the water-extracted Aβ peptides and/or to elucidate the exact nature of their N termini were not successful due to low yields and a number of co-purified and in part presumably amyloid-associated proteins that were detected with general protein stains, such as Coomassie Blue or Silver.

Aβ Patterns in APP23 Mouse Brains Exhibit Noticeable Differences to Human AD Brain Samples—For comparing the Aβ peptide variants in APP23 mice with human AD amyloid pathology, we subjected five human temporal lobe tissue samples to sequential extraction as described above. Three of the samples were from AD patients and two from age-matched nondemented controls with and without neuropathologically

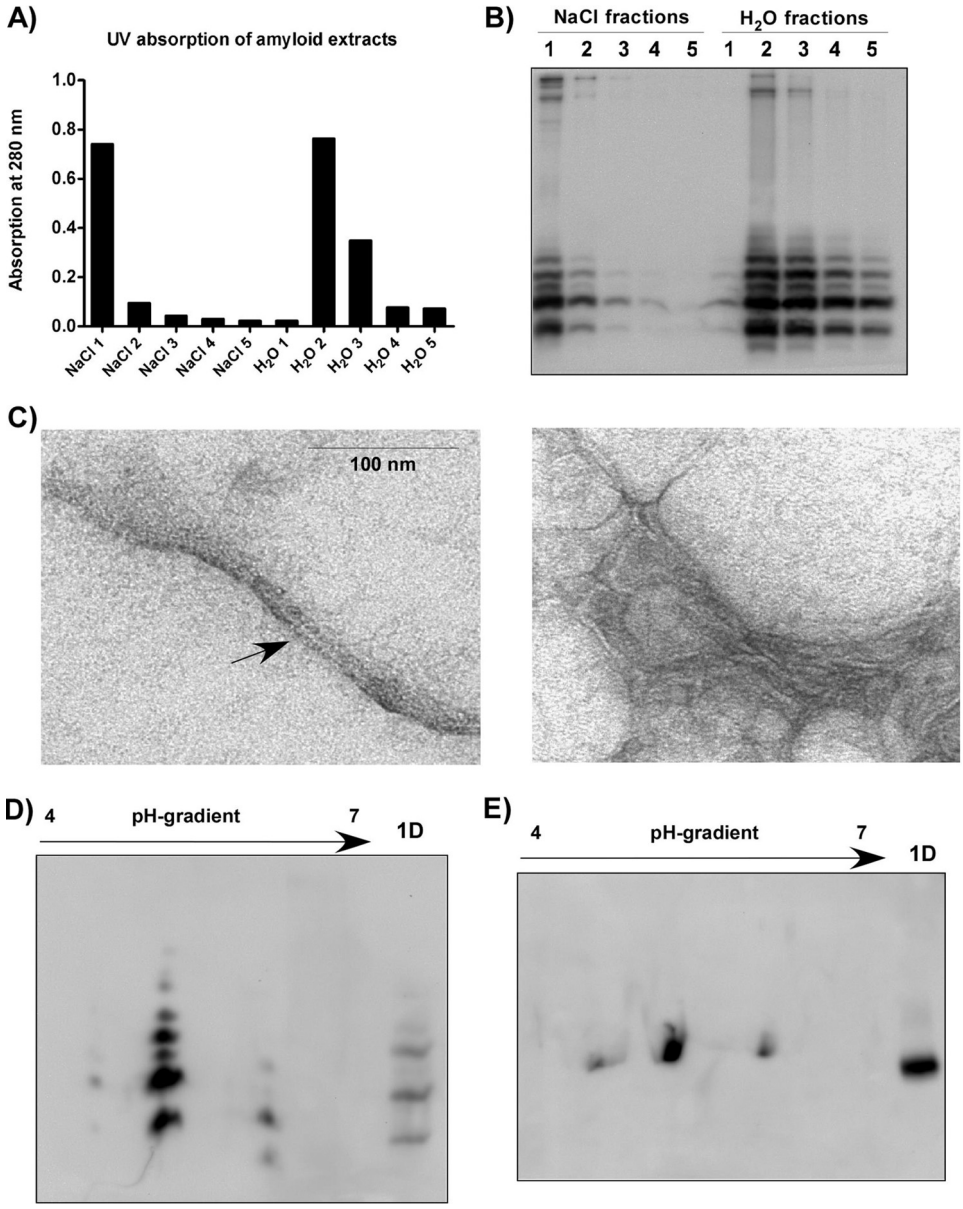

FIGURE 2. **Extraction of amyloid fibrils from the brain of a 24-month-old APP23 mouse with ultrapure water according to the method developed by Pras *et al.* (21).** *A,* UV absorption at 280 nm of the NaCl and H_2O fractions. *B,* Aβ peptides from the NaCl and H_2O fractions were separated by urea-SDS-PAGE followed by immunoblot with mAb 1E8. *C,* electron microscopic structure of the amyloid extracted in the second H_2O fraction. *Left panel,* material was fixated on a grid with 0.2% glutaraldehyde and stained with 2% uranyl acetate. Note the coiled structure of two intertwining fibrils as indicated by the *arrow*. *Right panel,* amyloid was precipitated on a grid with 10 mM $CaCl_2$ and stained with 1% phosphotungstic acid, pH 7.5. *D,* Aβ peptides from the second H_2O fraction were separated on a two-dimensional gel and detected by immunoblotting with 1E8. *E,* two-dimensional separation of water-extracted amyloid in the absence of urea and analyzed by 1E8 immunoblot.

confirmed amyloid deposits (Table 1). Aβ peptides were readily detected by immunoblot analysis in the detergent and formic acid fractions from all three AD samples and also in control sample NDC1 (amyloid stage B) (Fig. 3, *A* and *B*). The detergent and formic acid fractions from APP23 mice displayed fairly similar patterns of different Aβ variants. In both, Aβ(1–40) was clearly the most abundant species with minor amounts of co-deposited Aβ(1–37), -(1–38), -(1–39), and -(1–42). In all three human temporal lobe samples from AD patients and in NDC1, the predominant detergent-soluble Aβ peptide was Aβ(1–42) (Fig. 3*A*). The second most abundant Aβ variant in the AD samples co-migrated with synthetic Aβ(2–42). The formic acid preparations from the human tissue samples displayed substantial inter-individual differences. In sample AD1, the presumed Aβ(1–40) was the most prominent peptide followed by Aβ(1–42). In samples AD2, AD3, and NDC1, the most abundant Aβ peptide was Aβ(1–42) and was accompanied by varying amounts of additional Aβ peptides co-migrating with synthetic Aβ(1–40), Aβ(2–42), or Aβ(1–38) (Fig. 3*B*). The biochemical detection of appreciable amounts of Aβ in the control sample NDC1 confirms the neuropathological classification amyloid stage B (Table 1), which is characterized by medium densities of amyloid deposits in isocortical areas (37). In the second control, NDC2 (amyloid stage 0, see Table 1), Aβ peptides were below the detection sensitivity of direct immunoblotting (Fig. 3, *A* and *B*). For comparing the detergent fractions from NDC1 and

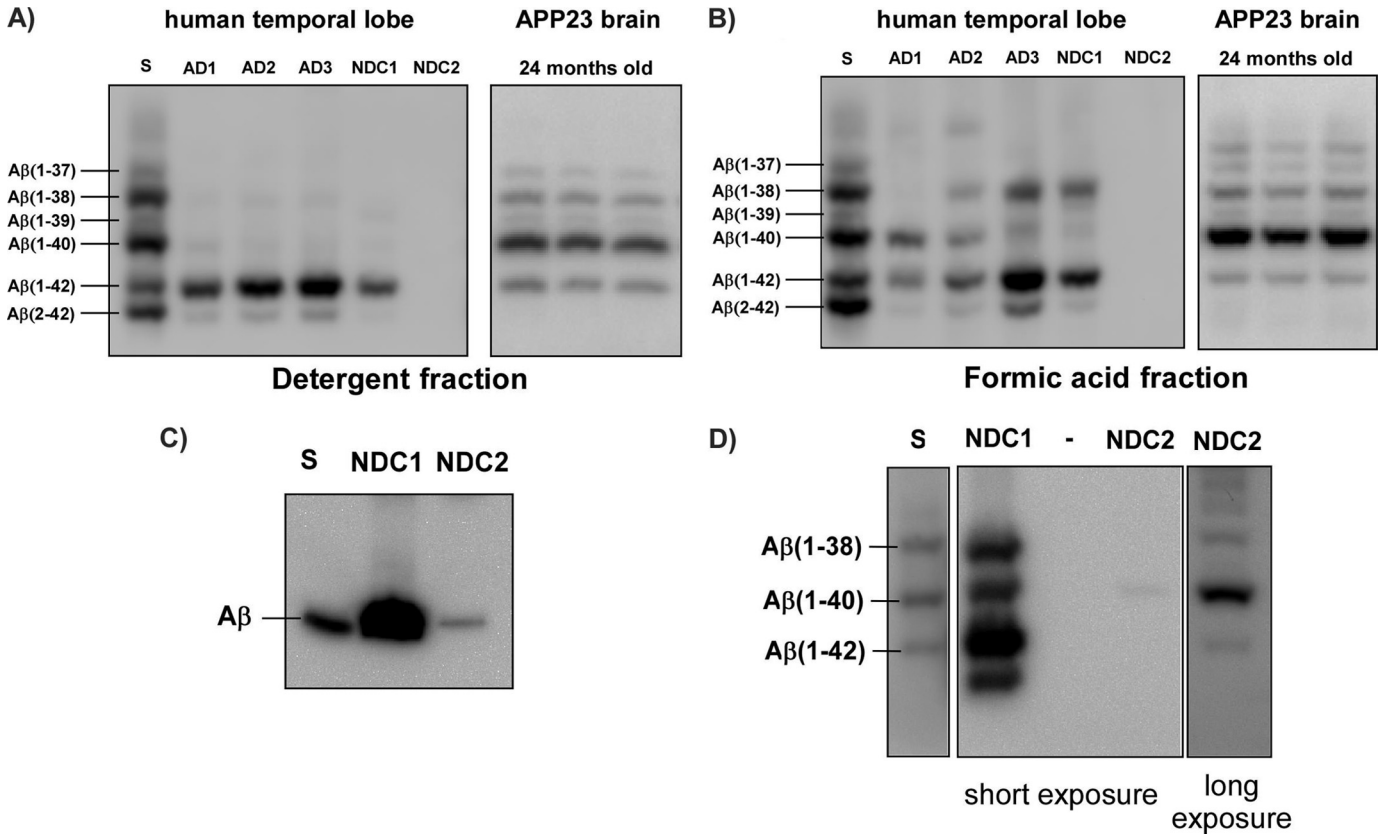

FIGURE 3. **Comparison of Aβ patterns between human and APP23 brain samples.** The relative abundance of different variants of Aβ in detergent and formic acid preparations from human temporal lobe samples and 24-month-old APP23 brains was analyzed by urea-SDS-PAGE/immunoblot. For comparison, the indicated synthetic Aβ peptides were loaded (*S*). *AD1, AD2,* and *AD3*, temporal lobe samples from three different AD patients; *NDC1* and *NDC2,* temporal lobe samples from nondemented controls neuropathologically classified as amyloid stage B and 0, respectively. *A,* Aβ immunoblots of the detergent fractions probed with mAb 1E8. For the human samples 500 ng and for the murine samples 100 ng of total protein of each was loaded. *B,* Aβ immunoblots of the formic acid fractions probed with mAb 1E8. 5 μl of a 1:1000 dilution (human samples) or 5 μl of a 1:10,000 dilution (mouse samples) were loaded. *C,* Aβ peptides from detergent fractions of NDC1 and NDC2 (6 mg of total protein each) were immunoprecipitated with mAb 1E8 and separated by Bicine/bis-Tris/Tris/sulfate SDS-PAGE followed by immunoblotting with mAb 1E8. Note that in the absence of urea the N- and C-terminal Aβ variants migrate in one band. *D,* C-terminal Aβ variants in immunoprecipitates from NDC1 and NDC2 were separated by urea-SDS-PAGE and visualized by immunoblot with mAb 1E8. For the visualization of NDC1 a short exposure time and for NDC2 a short and a long exposure time are shown. *S* = mixture of synthetic Aβ peptides.

NDC2, Aβ peptides were thus pre-enriched by immunoprecipitation prior to immunoblot analysis. Electrophoretic separation in the absence of urea indicated a comparatively low amount of total Aβ in NDC2, as expected (Fig. 3*C*). Most probably, this fraction represented a soluble pool of Aβ in this brain tissue sample devoid of amyloid deposits. Resolution of C-terminal Aβ variants by urea-SDS-PAGE revealed Aβ(1–40) to constitute the predominant Aβ species in NDC2 (Fig. 3*D*). In contrast, in NDC1 the most abundant Aβ variant was clearly Aβ(1–42), confirming the findings from direct immunoblot analysis (see above).

To provide further information regarding the relative abundance of N-truncated Aβ peptides in the APP23 mice as compared with an example of human AD amyloid pathology, we applied two-dimensional separation followed by immunoblotting with mAb 6E10. This antibody recognizes N-terminal Aβ variants from Aβ(1–42) to Aβ(5–42) (38). In the AD3 formic acid sample, a substantial proportion of the Aβ peptides displayed pI values greater than pH 6 suggesting N-terminal truncations. In contrast, only small amounts of corresponding N-truncated Aβ forms were observed in the murine sample (Fig. 4*A*). The most prominent N-terminal truncated Aβ peptide in human amyloid plaques starts with Glu-3 modified to pyrrolidone 2-carboxylic acid (pyroglutamate) (Aβ(N3pE)) (39, 40). Aβ(N3pE) was readily detected by immunoblotting with a specific antibody in the detergent and formic acid fractions from the human AD samples and also in the extracts from sample NDC1 (Fig. 4*B*). The modified peptides displayed higher electrophoretic mobilities than the Aβ peptides starting at Asp-1, and synthetic Aβ(N3pE40) was clearly resolved from Aβ(N3pE42). Reprobing of the blot with antibody 6E10 confirmed that the pyroglutamate-modified peptides represented a major fraction in the human AD samples (Fig. 4*B*, *bottom panel*). In the APP23 mice, we were able to detect multiple peptide bands with the Aβ(N3pE) antibody in formic acid extracts from 15- and 24-month-old mice when relative large protein amounts were applied (Fig. 4*C*). For appreciable signals with the Aβ(N3pE) antibody, ~1000 times more total protein was loaded on the gel than for detection of N-terminally unmodified peptides with antibody 1E8. Trace amounts of Aβ(N3pE) were also observed in the detergent fractions from 24-month-old mice (data not shown). From the band intensities on the blots and by comparison with dilutions of a synthetic Aβ(N3pE40) reference peptide, the amount of Aβ(N3pE) peptides in the murine formic acid fractions was estimated to be ~50 ± 14 pg/mg wet tissue (mean ± S.D., $n = 4$) at 15 months

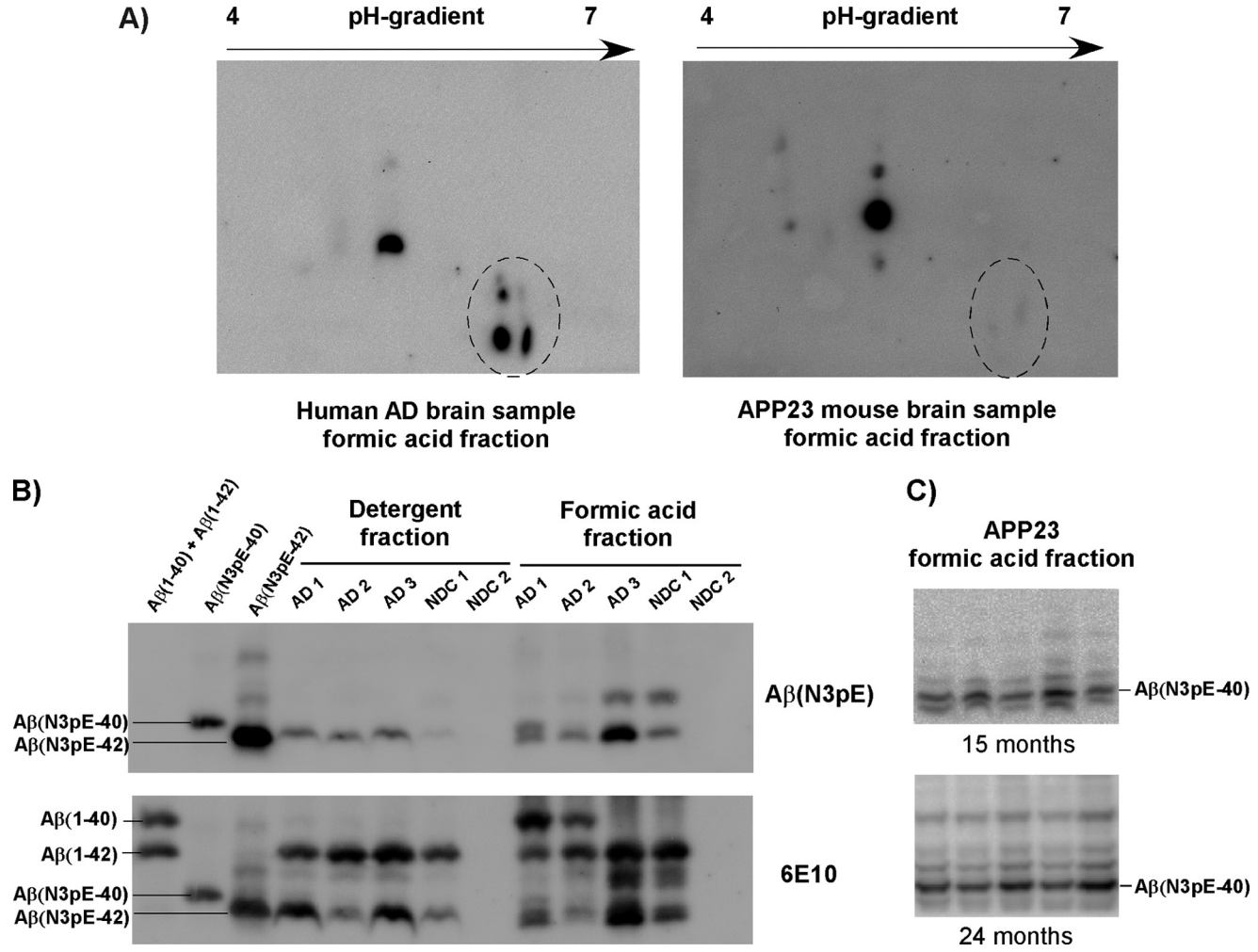

FIGURE 4. **N-truncated forms of Aβ are major components in human amyloid plaques but occur only in minor amounts in APP23 mice.** *A,* representative two-dimensional separation of Aβ peptides in formic acid fractions from sample AD3 and from a 24-month-old APP23 mouse. The immunoblots were probed with mAb 6E10. IPG strips with a linear pH gradient from 4 to 7 were used. Spots with pI values of >6, suggesting N-terminal truncation, are *encircled*. *B* and *C,* one-dimensional urea-SDS-PAGE immunoblots reveal that Aβ(N3pE) is highly abundant in human amyloid preparations, but it occurs only in minor amounts in APP23 mice. *B,* Aβ(N3pE) peptides in human samples. The blots were first probed with the polyclonal anti-Aβ(N3pE) antibody (*upper panel*). Afterward, the bound antibodies were removed with Restore™ Western blot Stripping Buffer (Thermo Scientific), and the blots were reprobed with the mAb 6E10 (*lower panel*). Synthetic Aβ peptides were loaded in the first three lanes: 500 pg of Aβ(1–40) and 500 pg of Aβ(1–42), 200 pg of Aβ(N3pE-40) and 200 pg of Aβ(N3pE-42). *C,* anti-Aβ(N3pE) immunoblots of samples from 15- and 24-month-old APP23 mice (formic acid-fractions).

and ~469 ± 138 pg/mg wet tissue (mean ± S.D., $n = 8$) at 24 months of age, respectively. Thus, Aβ(N3pE) increased with age in parallel with total Aβ and accounted for roughly 0.1% of the total Aβ in the formic acid fractions.

Aβ Variants in Aged APP51 Mice Overexpressing Wild Type APP—The findings presented so far revealed clear differences in terms of the composition of Aβ deposits between APP23 mice and human AD pathology. To explore whether these differences can be primarily attributed to the Swedish mutant form of APP overexpressed in the APP23 mice, we extended our study to the closely related APP51 mouse line, which is transgenic for human wild type APP (22). In APP51 mice, amyloid plaques appear between 12 and 15 month of age, which is ~6–9 months later than in the APP23 line (41). Detergent and formic acid brain fractions from 6-, 15-, and 24-month-old APP51 mice were prepared and analyzed as described for the APP23 mice. In pre-plaque, 6-month-old APP51 mice, only low levels of Aβ peptides could be detected. The total Aβ content increased dramatically between 15 and 24 months of age, resembling the exponential plaque growth observed in the APP23 line between ages 7 and 24 months (see above). Again, in detergent as well as in formic acid fractions, the predominant Aβ peptide was Aβ(1–40) (Fig. 5*A* and Table 4). Similar to the findings in APP23 mice, the relative contribution of Aβ(1–42) was comparatively high in the formic acid fractions at an early plaque state and decreased with ongoing amyloid deposition. The Aβ(1–42)/(1–40) ratio (rank sums) in the formic acid fractions was significantly lower in 24-month-old mice than in 15-month-old animals ($p < 0.01$) according to the nonparametric Kruskal-Wallis test with Dunn's multiple comparison post-test. A two-dimensional separation of a formic acid brain extract from a 24-month-old APP51 mouse indicated minor amounts of N-terminal truncated Aβ peptides (pI ~6.2) (Fig. 5*B*). Based on semi-quantitative image analysis from anti-Aβ(N3pE) immunoblots (Fig. 5*C*), we estimate Aβ(N3pE) to account for roughly 1% of total formic acid extracted Aβ in 24-month-old APP51 mice. This proportion is higher than in the APP23 line but still substantially below that in human AD samples (40).

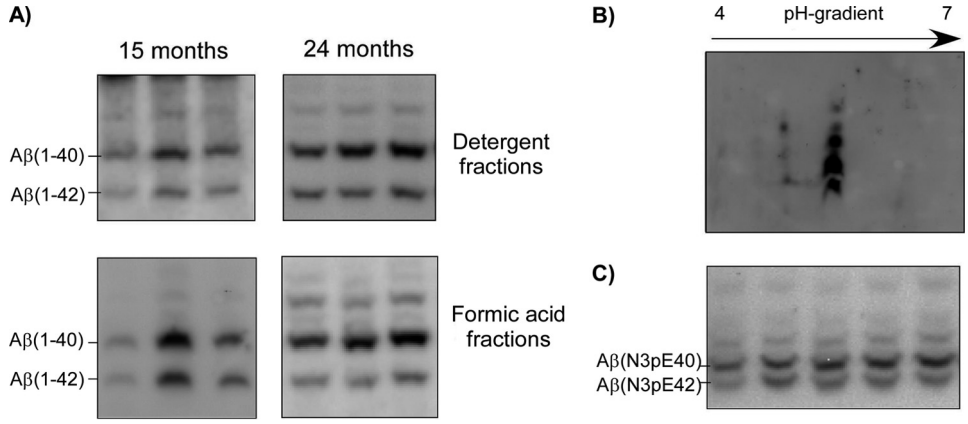

FIGURE 5. **Aβ peptide patterns in brains from APP51 mice overexpressing human wild type APP751.** *A,* representative Aβ peptide blots of detergent and formic acid fractions from brains of 15- and 24-month-old APP51 mice. Aβ peptides were separated by urea-SDS-PAGE followed by immunoblot with mAb 1E8. The total protein amount loaded for the different age groups was adjusted to obtain comparable signals on the blots. *B,* two-dimensional immunoblot of a formic acid fraction from the brain of a 24-month-old APP51 mouse, probed with mAb 6E10. *C,* Aβ(N3pE) peptides in formic acid fractions from the brains of 24-month-old APP51 mice. The blots were probed with the polyclonal anti-Aβ(N3pE) antibody.

TABLE 4

Aβ peptides in the detergent- and formic acid fractions from APP51 mouse brains

	Total Aβ (ng/mg wet tissue)[a]				Aβ(1–42)/(1–40) ratio			
	Detergent fraction		Formic acid fraction		Detergent fraction		Formic acid fraction	
Age	Median	25–75% percentile	Median	25–75% percentile	Median	25–75% percentile	Median	25–75% percentile
months								
6 (n = 5)	0.36	0.28–0.40	0.02	0.01–0.02	0.30	0.27–0.32	0.38	0.32–0.39
15 (n = 5)	0.73	0.70–1.18	0.07	0.07–0.25	0.47	0.45–0.49	0.62	0.45–0.71
24 (n = 5)	21.28	19–37	10.44	7.97–16.49	0.50	0.44–0.58	0.23	0.23–0.28

[a] Brain tissue samples were subjected to Aβ urea-SDS-PAGE followed by immunoblot with the mAb 1E8. The blots were run in duplicate, and the Aβ peptides were quantified by comparison with a dilution series of synthetic Aβ(1–40) standards. The values for the distinct Aβ variants were added to obtain total Aβ.

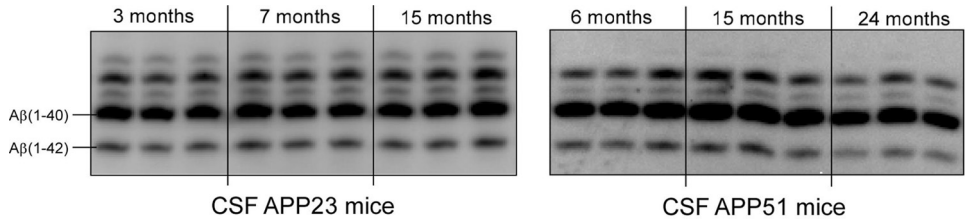

FIGURE 6. **Aβ patterns in CSF from APP23- and APP51 mice.** CSF samples were separated by urea-SDS-PAGE followed by immunoblot with mAb 1E8. Representative blots for each age group from APP23 and APP51 mice are shown.

Aβ Peptide Patterns in CSF—Aβ peptides in CSF from APP23 and related transgenic mice display a rapid turnover and appear to represent a pool of newly generated soluble Aβ in brain (41). In both transgenic mouse lines, patterns of 5 Aβ peptides were observed that were fairly similar to those reported for human CSF (11). In all cases, Aβ(1–40) represented the predominant species and was accompanied by Aβ peptides co-migrating with synthetic Aβ(1–37), -(1–38), -(1–39), and -(1–42) (Fig. 6). In the small number of CSF samples studied here, we did not observe statistically significant differences in the median total CSF Aβ levels or median Aβ(1–42)/(1–40) ratios between the tested age groups in either mouse line (Table 5). It is clear, however, that a substantially larger sample size will be required for an in-depth analysis able to reliably detect even subtle changes.

The overall mean total Aβ CSF levels in APP23 mice (independent of age) was 68 ± 10 ng/ml (mean ± S.D., n = 14) and 52 ± 18 ng/ml (n = 14) in APP51 mice. Thus, the mean total Aβ CSF concentration in APP transgenic mice was about 6-fold higher in APP23 and about 5-fold higher in APP51 mice than in human CSF analyzed in a comparable fashion (34). Two-dimensional immunoblot analysis with mAb 1E8 did not indicate the presence of appreciable amounts of additional Aβ species with pI values other than ~5.4 (data not shown).

DISCUSSION

We report here a comprehensive comparison of Aβ peptides extracted from the brains of APP23 transgenic mice before and after onset of brain amyloid deposition and human temporal lobe samples from individuals with and without neuropathologically confirmed amyloid plaques. In the transgenic mice, a massive accumulation of Aβ was observed between 7 and 24 months of age. The time course of amyloid deposition involving a lag phase of several months is in line with the suggested mechanism of nucleation-dependent polymerization for amyloid formation (42). The most abundant form of Aβ in both detergent and formic acid fractions from the brains of APP23 mice at all stages analyzed was Aβ(1–40). Additionally, the Aβ variants

TABLE 5

Aβ patterns in CSF samples from APP23 and APP51 mice

Aβ peptides were separated by urea-SDS-PAGE/immunoblot and probed with mAb 1E8. The Aβ peptides were quantified by comparison with a dilution series of synthetic Aβ(1–40) standards. The values for the distinct Aβ variants were added to obtain total Aβ. For each group, medians and 25–75% percentiles are shown.

	APP23						APP51					
	3 months		7 months		15 months		6 months		15 months		24 months	
Age (months)	Median	25–75% percentile	Median	25–75% percentile	Median	25–75% percentile	Median	25–75% percentile	Median	25–75% percentile	Median	25–75% percentile
Total Aβ (ng/ml)	63.4	54.8–77.3	67.4	64.0–80.2	69.7	66.8–87.0	45.1	38.8–59.3	74.2	40.9–86.7	40.9	39.0–46.5
Aβ(1–42)/(1–40)	0.19	0.16–0.20	0.21	0.16–0.22	0.19	0.16–0.21	0.13	0.12–0.14	0.10	0.09–0.11	0.10	0.10–0.14

Aβ(1–38), -(1–37), -(1–39), -(2–40), and -(3–40) and minor amounts of pyroglutamate-bearing (Aβ(N3pE)) forms and endogenous murine Aβ(1–40) were found to be co-deposited. A large excess of formic acid-soluble Aβ40 over Aβ42 in the cortex of 20-month-old APP23 mice has been reported before (43). The comparison of the amyloid preparations from APP23 transgenic mice with those from human AD brain samples revealed substantial differences in terms of the relative abundance of specific N- and C-terminal Aβ variants. In the human samples, Aβ(1–42), the presumed N-truncated Aβ(2/3–42) and Aβ(N3pE) peptides were much more prevalent than in the APP23 mice. N-truncated Aβ species were reported to account for more than 60% of the Aβ peptides in early and later stages of human AD amyloid pathology. Thus, N-truncated forms of Aβ ending at residue Ala-42 were proposed to be of particular importance in the development of AD neuropathology (44). In line with this hypothesis, in a human control brain sample devoid of amyloid plaques (amyloid stage 0), we observed a substantially different pattern of Aβ peptides than in the human brain samples classified as amyloid stages B or C. In the sample without plaques, the total amount of Aβ was comparatively small and presumably represented soluble Aβ. The predominant Aβ variant was Aβ(1–40), which is consistent with Aβ(1–40) representing the main soluble Aβ species in cell culture supernatants (9) and biological fluids (10, 11). Thus, the soluble Aβ species appear similar in humans and transgenic mice. The low abundance of Aβ(1–42), N-truncated Aβ(2/3–42), and Aβ(N3pE) we observed in the amyloid deposits in aged APP23 transgenic mice suggests differences in the underlying biochemical mechanism driving the amyloid deposition in transgenic mice as compared with human AD brain.

The Aβ(1–42)/(1–40) ratio in the mice was found to be relatively high in the formic acid brain extracts by 7 months of age, which represents an early plaque stage. Kinetic *in vitro* aggregation studies have revealed that Aβ(1–42) is more prone to aggregation than the shorter variants Aβ(1–40) and Aβ(1–39) and that amyloid formation by the kinetically soluble Aβ(1–40) can be nucleated by Aβ(1–42) (32). In APP24 transgenic mice, a related animal model overexpressing human APP carrying the Swedish K670N/M671L and the London V717I mutations, Aβ(1–42) was shown to be the Aβ variant initially deposited (41). Our findings suggest that once the amyloid fibril formation has been nucleated (possibly by Aβ(1–42)), the Aβ accumulation in APP23 transgenic mice is mainly driven by the elevated production and high abundance of the five main Aβ peptides Aβ(1–40), -(1–42), -(1–38), -(1–39), and -(1–37). Because of the large amounts of Aβ constantly being produced in the transgenic mice, the sustained Aβ deposition proceeds at a higher rate than in human AD brain, and differences between specific Aβ variants in their kinetic solubility or the ability to nucleate are thus probably less relevant. A correlation between interstitial Aβ concentration, as determined by *in vivo* microdialysis, and amyloid plaque growth has been demonstrated in APP/PS1 transgenic mice (45). Furthermore, in Tg2576 transgenic mice, the local interstitial Aβ concentrations in specific brain regions in young mice were recently reported to be associated with differences in the regional Aβ plaque burden in aged animals (46). In APP51 transgenic mice overexpressing human wild type APP, we observed patterns of deposited Aβ peptides fairly similar to those in the APP23 line. In both animal models, Aβ(1–40) was the predominant variant at all stages of plaque development analyzed. N-truncated forms and Aβ42 peptides were less abundant. Thus, the Swedish APP mutation does not provide an explanation for the observed differences in the brain Aβ patterns between aged APP23 mice and human AD pathology.

Two-dimensional gel electrophoresis indicated the presence of additional, modified Aβ peptides displaying acidic pI shifts in the amyloid preparations. We were able to identify *N*-formylation (+28) and *N*-carbamoylation (+43), which turned out to be artificially generated during the experimental procedures. These findings suggest that the primary amino group of Aβ is highly susceptible to artificial chemical modification and that extreme care must be taken during the analysis of Aβ peptide variants and potential post-translational modifications. A fraction of the Aβ peptides displaying an acidic pI shift was apparently unmodified, which might be explained by the following: (i) partially labile chemical modifications, (ii) the presence of conformational peptide variants (47) or oligomers, and (iii) tight interaction with distinct ampholyte molecules (48). Even when formic acid and urea were omitted from the work flow, these potential mechanisms also may have led to the appearance of residual Aβ peptides with low pI. As a relatively gentle approach to the preanalytical preparation of amyloid, we additionally employed "amyloid water extraction," a method originally introduced for the preparation of peripheral amyloid fibrils from a case of primary amyloidosis (20). The procedure has been successfully applied to the preparation of amyloid components from different sources (49–54). However, to the best of our knowledge, it has not been reported before in the context of studies on AD-type amyloid. We confirmed the presence of typical amyloid fibrils in the water extract from an APP23 mouse brain by negative staining and electron microscopy. Immunoblot analysis revealed patterns of Aβ peptides

similar to those in detergent and formic acids extracts. Taken together, these observations suggest that water extraction represents an approach devoid of harsh chemicals for the preparation of amyloid fibrils from animal models of AD amyloid neuropathology.

The Aβ peptides in CSF from APP23 transgenic mice undergo rapid turnover and appear to mirror newly generated soluble brain Aβ (41). Our semiquantitative immunoblot analysis indicated roughly 6- and 5-fold higher total CSF Aβ concentrations in APP23 and APP51 mice, respectively, compared with the reported levels in human CSF (34). In AD patients, CSF Aβ42 concentrations are inversely correlated with *in vivo* amyloid imaging load (13, 15). The selective reduction of Aβ42 in CSF may thus represent a direct biomarker of Aβ deposition in human brain possibly reflecting the preferential deposition of Aβ42. In the CSF samples from transgenic APP23 and APP51 mice analyzed here, we did not find evidence for statistically significant age-related or amyloid stage-related changes in the absolute Aβ CSF levels or in the relative distribution of the five C-terminal Aβ variants. It should be noted, however, that a larger sample size and additional time points will be required for an in-depth CSF analysis powerful enough to detect even subtle alterations.

Taken together, our findings reveal substantial differences in the Aβ peptide patterns between amyloid preparations from human AD temporal lobe samples and brains from two different APP transgenic mouse lines. The observations provide evidence for differences in the underlying molecular mechanisms driving the ongoing amyloid deposition in human AD brain and in the transgenic mouse models. This should be taken into consideration when translating observations from transgenic mice to the human disease.

Acknowledgments—We thank Heike Kamrowski-Kruck, Sabine Lehman, Lars van Werven, Thomas Liepold, Marina Uecker, and Dörte Hesse for expert technical support.

REFERENCES

1. Glenner, G. G., and Wong, C. W. (1984) *Biochem. Biophys. Res. Commun.* **120,** 885–890
2. Masters, C. L., Simms, G., Weinman, N. A., Multhaup, G., McDonald, B. L., and Beyreuther, K. (1985) *Proc. Natl. Acad. Sci. U.S.A.* **82,** 4245–4249
3. Delacourte, A., and Defossez, A. (1986) *J. Neurol. Sci.* **76,** 173–186
4. Grundke-Iqbal, I., Iqbal, K., Tung, Y. C., Quinlan, M., Wisniewski, H. M., and Binder, L. I. (1986) *Proc. Natl. Acad. Sci. U.S.A.* **83,** 4913–4917
5. Kosik, K. S., Joachim, C. L., and Selkoe, D. J. (1986) *Proc. Natl. Acad. Sci. U.S.A.* **83,** 4044–4048
6. Selkoe, D. J. (1998) *Trends Cell Biol.* **8,** 447–453
7. Vassar, R., Kovacs, D. M., Yan, R., and Wong, P. C. (2009) *J. Neurosci.* **29,** 12787–12794
8. Bergmans, B. A., and De Strooper, B. (2010) *Lancet Neurol.* **9,** 215–226
9. Asami-Odaka, A., Ishibashi, Y., Kikuchi, T., Kitada, C., and Suzuki, N. (1995) *Biochemistry* **34,** 10272–10278
10. Lewczuk, P., Esselmann, H., Bibl, M., Paul, S., Svitek, J., Miertschischk, J., Meyrer, R., Smirnov, A., Maler, J. M., Klein, C., Otto, M., Bleich, S., Sperling, W., Kornhuber, J., Rüther, E., and Wiltfang, J. (2004) *Electrophoresis* **25,** 3336–3343
11. Wiltfang, J., Esselmann, H., Bibl, M., Smirnov, A., Otto, M., Paul, S., Schmidt, B., Klafki, H. W., Maler, M., Dyrks, T., Bienert, M., Beyermann, M., Rüther, E., and Kornhuber, J. (2002) *J. Neurochem.* **81,** 481–496
12. Jarrett, J. T., and Lansbury, P. T., Jr. (1993) *Cell* **73,** 1055–1058
13. Fagan, A. M., Mintun, M. A., Mach, R. H., Lee, S. Y., Dence, C. S., Shah, A. R., LaRossa, G. N., Spinner, M. L., Klunk, W. E., Mathis, C. A., DeKosky, S. T., Morris, J. C., and Holtzman, D. M. (2006) *Ann. Neurol.* **59,** 512–519
14. Jack, C. R., Jr., Knopman, D. S., Jagust, W. J., Shaw, L. M., Aisen, P. S., Weiner, M. W., Petersen, R. C., and Trojanowski, J. Q. (2010) *Lancet Neurol.* **9,** 119–128
15. Grimmer, T., Riemenschneider, M., Förstl, H., Henriksen, G., Klunk, W. E., Mathis, C. A., Shiga, T., Wester, H. J., Kurz, A., and Drzezga, A. (2009) *Biol. Psychiatry* **65,** 927–934
16. Klafki, H. W., Staufenbiel, M., Kornhuber, J., and Wiltfang, J. (2006) *Brain* **129,** 2840–2855
17. Citron, M. (2010) *Nat. Rev. Drug Discov.* **9,** 387–398
18. Sturchler-Pierrat, C., Abramowski, D., Duke, M., Wiederhold, K. H., Mistl, C., Rothacher, S., Ledermann, B., Bürki, K., Frey, P., Paganetti, P. A., Waridel, C., Calhoun, M. E., Jucker, M., Probst, A., Staufenbiel, M., and Sommer, B. (1997) *Proc. Natl. Acad. Sci. U.S.A.* **94,** 13287–13292
19. Elder, G. A., Gama Sosa, M. A., and De Gasperi, R. (2010) *Mt. Sinai J. Med.* **77,** 69–81
20. Andrä, K., Abramowski, D., Duke, M., Probst, A., Wiederhold, K. H., Bürki, K., Goedert, M., Sommer, B., and Staufenbiel, M. (1996) *Neurobiol. Aging* **17,** 183–190
21. Pras, M., Schubert, M., Zucker-Franklin, D., Rimon, A., and Franklin, E. C. (1968) *J. Clin. Invest.* **47,** 924–933
22. Bodendorf, U., Danner, S., Fischer, F., Stefani, M., Sturchler-Pierrat, C., Wiederhold, K. H., Staufenbiel, M., and Paganetti, P. (2002) *J. Neurochem.* **80,** 799–806
23. Klafki, H. W., Pick, A. I., Pardowitz, I., Cole, T., Awni, L. A., Barnikol, H. U., Mayer, F., Kratzin, H. D., and Hilschmann, N. (1993) *Biol. Chem. Hoppe-Seyler* **374,** 1117–1122
24. Wiltfang, J., Arold, N., and Neuhoff, V. (1991) *Electrophoresis* **12,** 352–366
25. Klafki, H. W., Wiltfang, J., and Staufenbiel, M. (1996) *Anal. Biochem.* **237,** 24–29
26. Wiltfang, J., Smirnov, A., Schnierstein, B., Kelemen, G., Matthies, U., Klafki, H. W., Staufenbiel, M., Hüther, G., Rüther, E., and Kornhuber, J. (1997) *Electrophoresis* **18,** 527–532
27. Maler, J. M., Klafki, H. W., Paul, S., Spitzer, P., Groemer, T. W., Henkel, A. W., Esselmann, H., Lewczuk, P., Kornhuber, J., and Wiltfang, J. (2007) *Proteomics* **7,** 3815–3820
28. Schieb, H., Spitzer, P., Riess, V., Wiltfang, J., and Klafki, H. W. (2010) *Proteomics* **10,** 3539–3543
29. Ida, N., Hartmann, T., Pantel, J., Schröder, J., Zerfass, R., Förstl, H., Sandbrink, R., Masters, C. L., and Beyreuther, K. (1996) *J. Biol. Chem.* **271,** 22908–22914
30. Wiltfang, J., Esselmann, H., Cupers, P., Neumann, M., Kretzschmar, H., Beyermann, M., Schleuder, D., Jahn, H., Rüther, E., Kornhuber, J., Annaert, W., De Strooper, B., and Saftig, P. (2001) *J. Biol. Chem.* **276,** 42645–42657
31. Candiano, G., Bruschi, M., Musante, L., Santucci, L., Ghiggeri, G. M., Carnemolla, B., Orecchia, P., Zardi, L., and Righetti, P. G. (2004) *Electrophoresis* **25,** 1327–1333
32. Jarrett, J. T., Berger, E. P., and Lansbury, P. T., Jr. (1993) *Biochemistry* **32,** 4693–4697
33. Güntert, A., Döbeli, H., and Bohrmann, B. (2006) *Neuroscience* **143,** 461–475
34. Bibl, M., Mollenhauer, B., Esselmann, H., Lewczuk, P., Klafki, H. W., Sparbier, K., Smirnov, A., Cepek, L., Trenkwalder, C., Rüther, E., Kornhuber, J., Otto, M., and Wiltfang, J. (2006) *Brain* **129,** 1177–1187
35. Cohen, A. S., and Calkins, E. (1959) *Nature* **183,** 1202–1203
36. Shirahama, T., and Cohen, A. S. (1967) *J. Cell Biol.* **33,** 679–708
37. Braak, H., and Braak, E. (1991) *Acta Neuropathol.* **82,** 239–259
38. Vanderstichele, H., De Meyer, G., Andreasen, N., Kostanjevecki, V., Wallin, A., Olsson, A., Blennow, K., and Vanmechelen, E. (2005) *Clin. Chem.* **51,** 1650–1660
39. Saido, T. C., Iwatsubo, T., Mann, D. M., Shimada, H., Ihara, Y., and Kawashima, S. (1995) *Neuron* **14,** 457–466
40. Kuo, Y. M., Emmerling, M. R., Woods, A. S., Cotter, R. J., and Roher, A. E. (1997) *Biochem. Biophys. Res. Commun.* **237,** 188–191

41. Abramowski, D., Wiederhold, K. H., Furrer, U., Jaton, A. L., Neuenschwander, A., Runser, M. J., Danner, S., Reichwald, J., Ammaturo, D., Staab, D., Stoeckli, M., Rueeger, H., Neumann, U., and Staufenbiel, M. (2008) *J. Pharmacol. Exp. Ther.* **327,** 411–424
42. Harper, J. D., and Lansbury, P. T., Jr. (1997) *Annu. Rev. Biochem.* **66,** 385–407
43. Kuo, Y. M., Beach, T. G., Sue, L. I., Scott, S., Layne, K. J., Kokjohn, T. A., Kalback, W. M., Luehrs, D. C., Vishnivetskaya, T. A., Abramowski, D., Sturchler-Pierrat, C., Staufenbiel, M., Weller, R. O., and Roher, A. E. (2001) *Mol. Med.* **7,** 609–618
44. Sergeant, N., Bombois, S., Ghestem, A., Drobecq, H., Kostanjevecki, V., Missiaen, C., Wattez, A., David, J. P., Vanmechelen, E., Sergheraert, C., and Delacourte, A. (2003) *J. Neurochem.* **85,** 1581–1591
45. Yan, P., Bero, A. W., Cirrito, J. R., Xiao, Q., Hu, X., Wang, Y., Gonzales, E., Holtzman, D. M., and Lee, J. M. (2009) *J. Neurosci.* **29,** 10706–10714
46. Bero, A. W., Yan, P., Roh, J. H., Cirrito, J. R., Stewart, F. R., Raichle, M. E., Lee, J. M., and Holtzman, D. M. (2011) *Nat. Neurosci.* **14,** 750–756
47. Lutter, P., Meyer, H. E., Langer, M., Witthohn, K., Dormeyer, W., Sickmann, A., and Blüggel, M. (2001) *Electrophoresis* **22,** 2888–2897
48. Schaefer, H., Chamrad, D. C., Herrmann, M., Stuwe, J., Becker, G., Klose, J., Blueggel, M., Meyer, H. E., and Marcus, K. (2006) *Biochim. Biophys. Acta* **1764,** 1948–1962
49. Sletten, K., Husby, G., and Natvig, J. B. (1976) *Biochem. Biophys. Res. Commun.* **69,** 19–25
50. Sletten, K., Westermark, P., and Natvig, J. B. (1976) *J. Exp. Med.* **143,** 993–998
51. Westermark, P., and Sletten, K. (1982) *Clin. Exp. Immunol.* **49,** 725–731
52. Westermark, P., Sletten, K., Pitkänen, P., Natvig, J. B., and Lindholm, C. E. (1982) *Mol. Immunol.* **19,** 447–450
53. Klafki, H. W., Kratzin, H. D., Pick, A. I., Eckart, K., Karas, M., and Hilschmann, N. (1992) *Biochemistry* **31,** 3265–3272
54. Lundmark, K., Westermark, G. T., Nyström, S., Murphy, C. L., Solomon, A., and Westermark, P. (2002) *Proc. Natl. Acad. Sci. U.S.A.* **99,** 6979–6984
55. Braak, H., and Braak, E. (1995) *Neurobiol Aging* **16,** 271–278; discussion 278–284